

Biophysical Studies on Bone Cement Composites Based on Polyester Fumarate

N. A. Kamel,¹ T. H. Abou-Aiaad,¹ B. A. Iskander,² S. K. H. Khalil,³ S. H. Mansour,⁴
S. L. Abd-El-Messieh,¹ K. N. Abd-El-Nour¹

¹Microwave Physics and Dielectrics Department, National Research Centre, Dokki Cairo, Egypt

²Engineering Department, American University, Cairo, Egypt

³Spectroscopy Department, National Research Centre, Dokki, Cairo, Egypt

⁴Polymers and Pigments Department, National Research Centre, Dokki, Cairo, Egypt

Received 20 May 2009; accepted 6 October 2009

DOI 10.1002/app.31571

Published online 10 December 2009 in Wiley InterScience (www.interscience.wiley.com).

ABSTRACT: Polypropylene fumarate (PPF) as unsaturated linear polyester crosslinked with three different monomers namely *N*-vinyl pyrrolidone (NVP), methyl methacrylate (MMA), and a mixture of NVP/MMA (1 : 1 weight ratio) were prepared. The chemical structure of the PPF was characterized by means of ¹H-NMR, FTIR, as well as GPC. The mixture of PPF resin with the crosslinking monomers filled with (60, 65, and 70 wt %) of gypsum were also prepared as bone cement composites. The dielectric measurements carried out on these prepared samples at frequency range from 100 Hz–100 kHz indicate that the permittivity ϵ' and dielectric loss ϵ'' follow the order NVP > NVP/MMA > MMA. Both parameters were found to decrease by increasing the percentage of gypsum. According to Fröhlich and Havriliak Nagami functions, the relaxation times obtained could be attributed, respectively, to Maxwell-Wagner effect and to the relaxation process related to carboxyl, hydroxyl, and ester

functions associated with main chain. The latter relaxation time was found to increase by increasing gypsum content, whereas the electrical conductivity was found to decrease. The mechanical data of the investigated samples containing 60 wt % gypsum is characterized by the best properties and the behavior of the composites follows the order found in the case of dielectric properties (NVP > NVP/MMA > MMA). Formation of carbonate apatite of composite samples loaded with 60 wt % gypsum after immersing the samples for 4 weeks in simulated body fluid (SBF) was confirmed by the dielectric measurements and FTIR spectroscopy. In addition, the weight loss and the mechanical properties for such systems were also studied. © 2009 Wiley Periodicals, Inc. *J Appl Polym Sci* 116: 876–885, 2010

Key words: bone cement; polyester fumarate; composites; biophysical; dielectric relaxation; FTIR

INTRODUCTION

The field of biodegradable polymers is a fast growing area of polymer science because of the interest of such compounds for temporary surgical and pharmacological applications.¹ Aliphatic polyesters are the most attractive and promising among polymers degradable in model aqueous media or in animal bodies.

One polymer that is being investigated as an injectable and biodegradable bone cement is polypropylene fumarate (PPF).^{2,3} PPF is unsaturated linear polyester that can crosslink with itself or with a crosslinking agent such as *N*-vinyl pyrrolidone (NVP) and methyl methacrylate (MMA) or their mixture *in situ* to form a degradable polymeric network.^{3–8} Such *in situ* crosslinking of PPF was valuable for developing injectable materials that could fill skeletal defects of varying size and shape. As cured-

PPF matrices have high mechanical strength, the polymer has been especially promising for orthopedic application.⁹ In addition to its high mechanical strength, the possible biodegradation of PPF into nontoxic propylene glycol and fumaric acid is advantageous for designing biomaterials. On the basis of these unique properties, PPF has been formulated as bone cement,^{10–12} orthopedic scaffold for bone tissue regeneration,¹³ and a drug delivery system.^{14,15}

Dielectric spectroscopy is considered to be a powerful tool for studying the dynamics of polymers in a wide range of frequency. The different regimes of the dielectric spectra could be detected and the dynamics of the first and second relaxations can be obtained.¹⁶ Henry et al. studied the evolution of poly(lactic acid) degradability by dielectric spectroscopy measurements.¹⁶ This study led to the conclusion that Dielectric spectroscopy measurements made a new contribution to understand the dynamics of degradation of PLA. In particular, as the capacitance of a dielectric sample is inversely proportional to its thickness, is highly suitable for studies of thin films, in contrast with other techniques.

A series of crosslinkable nanocomposites has been developed using hydroxyapatite (HA) nanoparticles

Correspondence to: S. L. Abd-El-Messieh (slabdelmessieh@yahoo.com).

and poly(propylene fumarate) (PPF). PPF/HA nanocomposites with four different weight fractions of HA nanoparticles have been characterized in terms of thermal and mechanical properties.³ This investigation indicates that crosslinkable PPF/HA nanocomposites are useful for hard tissue replacement because of excellent mechanical strength and osteoconductivity.

Jayabalan¹⁷ concentrates his study on the preparation and characterization of Poly(propylene fumarate-co-caprolactone diol) thermoset composites with the aim to develop biodegradable bone fixation devices.

The aim of this work is to develop some composites based on fumarate polyester (polypropylene fumarate) as a biodegradable material with different crosslinking agents (*N*-vinyl pyrrolidone, methyl methacrylate, and a mixture of both (1 : 1 weight ratio) loaded with different concentrations of gypsum to be used as bone cements. The formation of carbonate apatite which is expected to take place by immersing the investigated samples in SBF solution will be studied by the dielectric relaxation and FTIR spectroscopy in addition to mechanical properties.

EXPERIMENTAL

Materials

Diethyl fumarate, 1,2-propanediol, and tetrabutyl titanate as the transesterification catalyst were reagent grade from Merck, Darmstadt, Germany, and used as received. *N*-vinyl pyrrolidone (NVP; freshly distilled) or methyl methacrylate (MMA; freshly distilled) were obtained from Merck, Darmstadt, Germany. Benzoyl peroxide, *N,N*-dimethyl-4-toluidine and gypsum [calcium sulfate dehydrate (CaSO₂.2H₂O)] were obtained from Aldrich.

Synthesis of fumarate polyester resin

Polypropylene fumarate (PPF) was prepared by the two-stage melt polycondensation method (esterification and polycondensation).⁶ A three-necked flask equipped with a condenser, nitrogen inlet tube, and magnetic stirrer was charged with (1 mol) diethyl fumarate and (2.2 mol) 1,2-propanediol and catalyst. The reaction mixture was heated to 150°C for 3 h. This first step (esterification) is considered to be completed after the collection of theoretical amount of ethanol, which was removed from the reaction mixture by distillation and collected in a graduate cylinder. In the second step of the transesterification of bis(hydroxypropyl), fumarate was carried out by heating the vessel at 200°C for 4 h, producing PPF and 1,2 propanediol as a by-product. The mixture was dissolved in methylene chloride and precipi-

tated in diethyl ether. The ether phase was decanted and the product was vacuum dried at room temperature to remove any remaining solvents.

Crosslinking of the prepared fumarate polyester

Fumarate polyester resin (PPF) was crosslinked with 30% by weight of *N*-vinyl pyrrolidone (NVP) or methylmethacrylate (MMA) monomer or a mixture of NVP/MMA in the ratio of 1 : 1 by weight using benzoyl peroxide as initiator (2% w/w). *N,N*-dimethyl-4-toluidine (0.2%) was added with rapid stirring; then, the mixture was molded using appropriate molds for different tests. Curing occurred after leaving the mixtures at room temperature (25°C) for 24 h.

Polymeric composites

The composites were prepared by mixing different ratios of gypsum (60, 65, and 70 wt %) with a mixture of fumarate polyester resin and crosslinking agents namely NVP, MMA, and NVP/MMA. The samples were left for 24 h at 25°C for curing.

Hydrolytic degradation

Crosslinked polyester and its composites were immersed in SBF solution pH 7.3 in an incubator at 37°C. Reagents used for SBF formulation are listed in Table I.¹⁸ To determine the weight loss during degradations, preweighed disks (5 cm diameter and 4 mm thickness) were each placed into a tared scintillation vial. Periodically, the samples were removed from the incubator, rinsed with distilled water, and dried in vacuum until a constant weight is reached. The mass loss was recorded as the average of the three individual degraded samples after immersion. The percentage of weight loss was determined for each sample by comparing the dry weight (m_d) remaining at specific time with the initial weight (m_o).

$$\% \text{ weight loss} = \frac{(m_o - m_d)}{m_o} \times 100 \quad (1)$$

Techniques

Infrared spectra were recorded by a JASCO FT/IR 300 E Fourier Transform Infrared (FTIR) Spectrometer (Tokyo, Japan).

Nuclear magnetic resonance (¹H-NMR) spectrum was run at 260 MCPS on a Jeol-Ex-270 NMR Spectrometer (Tokyo, Japan).

Molecular weight determination was done by gel permeation chromatography (GPC). GPC was carried out using Agilent Technologies Walden Bornn, Germany 1100 series equipped with two Styragel columns (10² and 10³ Å) and Refractive Index

TABLE I
Reagents for Preparation of the Simulated Body Fluid (SBF) Fluid (pH 7.3, 1L)

Order	Reagents	Amount
1	NaCl	7.996 g
2	NaHCO ₃	0.350 g
3	KCl	0.224 g
4	K ₂ HPO ₄ ·3H ₂ O	0.228 g
5	MgCl ₂ ·6H ₂ O	0.305 g
6	1M HCl	40 mL
7	CaCl ₂	0.278 g
8	Na ₂ SO ₄	0.071 g
9	(CH ₂ OH) ₃ CNH ₂	6.057 g

detector (Agilent G 1362). Tetrahydrofuran (THF) was used as eluent of flow rate of 1 mL min⁻¹. The columns were calibrated by means of polystyrene (an internal standard was used).

Dielectric measurements were carried out in the frequency range 100 Hz up to 100 kHz using an LCR meter type AG-411 B (Ando electric, Japan). The capacitance *C*, loss tangent tan δ , and ac resistance *R*_{ac} were measured directly from the bridge from which the permittivity ϵ' , dielectric loss ϵ'' , and *R*_{dc} were determined. A guard ring capacitor type NFM/5T Wiss Tech. Werkstätten (WTW) GMBH Germany was used as a measuring cell. The cell was calibrated using standard materials and the experimental error in ϵ' and ϵ'' were found to be $\pm 3\%$ and $\pm 5\%$, respectively.¹⁹ The temperature was controlled to 30°C by putting the cell in a digital oven and the experimental error in the temperature was $\pm 0.1^\circ\text{C}$.

The compressive tests were conducted according to ASTM D 695–ISO 604. The cylindrical specimens were prepared for compression test with aspect ratio 2 : 1 (length to diameter ratio). Hounsfield (100 KN) universal testing machine was used. Axial compressive load was applied to the specimen with head speed 3 mm/min.

The tensile tests were conducted according to the ASTM D638-03 and ISO 527-1. The mentioned machine specifications were used with the same speed after gripping the specimen for tensile test. The load-extension diagrams were plotted during the test and the mechanical properties were calculated.

RESULTS AND DISCUSSION

Characterization of PPF

The chemical structure of the prepared polyester was characterized by ¹H-NMR spectroscopy. ¹H-NMR spectrum of fumarate polyester (Fig. 1) contains a characteristic peaks at δ 1.3, 3.5, and 4.8 ppm attributed to methyl, methylene, and methane protons of propylene glycol, respectively. The

unsymmetrical signals at δ 6.5–6.8 seem to be two ill-defined doublets for the two olefinic protons of fumaric acid moiety. The polyester was further characterized by GPC crudely with THF as the solvent and linear polystyrene as the standard. The result showed that fumarate polyester possessed number average molecular weight (*M*_n) of 1729 g/mol and polydispersity of 1.53.

Dielectric spectroscopy measurements

The frequency dependence of the permittivity ϵ' and dielectric loss ϵ'' over the frequency range from 100 Hz–100 kHz and at 30°C for polypropylene fumarate (PPF) crosslinked with different crosslinking agents (NVP, MMA, and [NV/MMA (1 : 1 ratio)]) is presented in Figure 2. From this figure, it can be seen that ϵ' for all investigated samples decreases with increasing the frequency, which shows anomalous dispersion. On the other hand, the absorption curves of ϵ'' versus the frequency *f* shown in Figure 2 are broad indicating that more than one relaxation mechanism is present. It is also clear that the values of ϵ' and ϵ'' increase in the order MMA < NVP/MMA < NVP. This is may be due to the higher polarity of NVP (4D)²⁰ compared with that of MMA (1.79D).²¹

Example of the analyses is given in Figure 3 for polypropylene fumarate (PPF) crosslinked with different crosslinking agents. From this figure, an absorption region is detected at lower frequency range which is fitted by Fröhlich function²² with distribution parameter *p* = 3 and relaxation time ranging from to 3.2 to 3.8 × 10⁻⁴ s. The relaxation time associated with such process is found to be independent on the type of the monomer used for

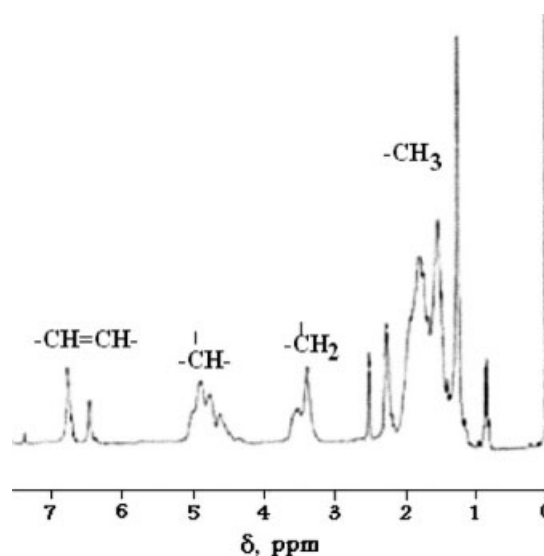


Figure 1 ¹H-NMR spectrum for the fumarate polyester resin (PPF).

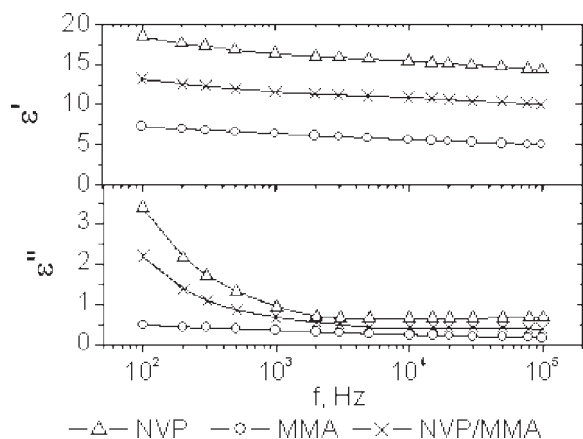


Figure 2 Permittivity ϵ' and dielectric loss ϵ'' for PPF crosslinked with NVP, MMA, and NVP/MMA.

crosslinking. This absorption region could be attributed to Maxwell-Wagner effect²² as it is expected to be at the lower frequency range due to the multiconstituents of the investigated systems. The experimental error of τ_1 was $\pm 2\%$.

The second absorption region in the higher frequency range could be associated with some local molecular motions rather than the main chain motion as it is expected to be frozen because the measurements were carried out at 30°C , i.e., lower than the glass transition T_g of the crosslinked polyester.²³ This relaxation corresponds to the terminal polar groups, carboxyl and hydroxyl functions, and to ester functions in the polymer chain.²⁴ The relaxation time associated with this region is found to be highly affected by the type of crosslinking agent and follows the order $\text{MMA} > \text{NVP/MMA} > \text{NVP}$, i.e., depending on the molar volume of the rotating units and consequently on the relaxation time.

The permittivity ϵ' and dielectric loss ϵ'' were also measured for the crosslinked polyester and its composites loaded with different ratios of gypsum (60, 65, and 70 wt %), respectively. Example of the obtained data is given in Figure 4. From this figure, it is seen that both ϵ' and ϵ'' decreases by increasing the filler content. The relationship between ϵ'' and the f were analyzed in the same way as discussed earlier to give two relaxation mechanisms through Fröhlich and Havriliak-Negami functions in addition to the conductivity term. The first relaxation time which ascribes Maxwell-Wagner effect is found to be independent on either the crosslinking monomer type or the filler content and found to ranging from 3.8 to 4×10^{-4} s. The second relaxation time τ_2 , ascribing the local molecular motions together with its relaxation strength S_2 in addition to the conductivity are listed in Table II. The experimental error in both of τ_2 and S_2 was found to be $\pm 2\%$.

From this table, it is notable that by increasing the filler content, the values of the relaxation time τ_2 increases, whereas the electrical conductivity σ and the relaxation strength S_2 decreases.

On the other hand, from this table, it is deduced that the previous properties τ_2 , σ , and S_2 for the samples crosslinked with NVP and mixture of MMA/NVP are not linearly fitted. This nonlinearity, which is noticed throughout the whole-investigated

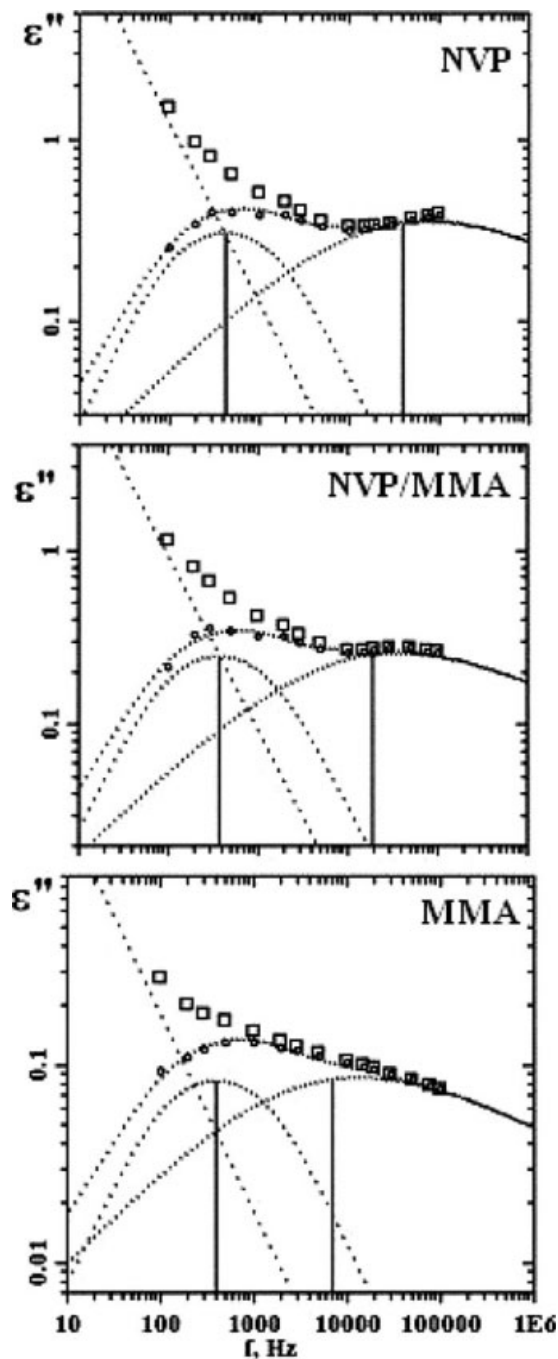


Figure 3 The analyses of ϵ'' data for PPF crosslinked with NVP, MMA, and NVP/MMA. Fitting the experimental data after subtraction of the losses due to dc conductivity with Fröhlich and Havriliak Negami functions.

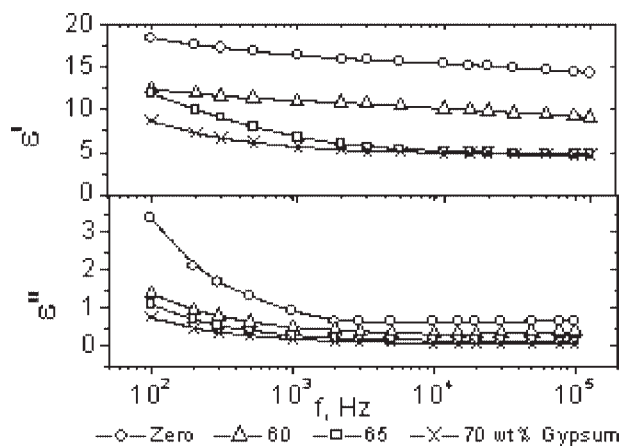


Figure 4 Permittivity ϵ' and dielectric loss ϵ'' for PPF crosslinked with NVP and loaded with gypsum.

systems containing the different percentages of gypsum, exhibits additional molecular order in case of crosslinked sample with NVP/MMA. This deviation could be attributed to some sort of molecular interaction between MMA and NVP which is expected to take place. This proposed interaction could lead to an increase in the molar volume and consequently the relaxation time.²¹ This result finds further justification through the conductivity measurements as well as the relaxation strength.

After immersing the crosslinked samples without filler and those containing 60 wt % gypsum in SBF solution for 4 weeks, the permittivity ϵ' and dielectric loss ϵ'' were measured. The data obtained after immersing in SBF are compared with those obtained before immersing and example of the data is shown in Figure 5. From this figure, it is seen that both ϵ' and ϵ'' decreases by immersing in the SBF solution. This decrease could be due to the formation of apatite structure that takes some ions to crystal forma-

TABLE II
Dielectric Parameters of the Composites Under Investigations

Gypsum wt %	$\sigma \Omega^{-1} \text{cm}^{-1} \times 10^{11}$	$\tau_2 \times 10^5 \text{ s}$	S_2
NVP			
0	19.50	0.74	4.32
60	6.93	0.80	2.24
65	5.96	0.84	0.93
70	4.06	1.03	0.51
NVP/MMA			
0	13.00	1.50	2.5
60	5.10	1.65	1.63
65	3.32	1.70	0.63
70	2.02	1.80	0.31
MMA			
0	1.65	3.33	1.29
60	1.30	3.50	0.55
65	0.96	3.79	0.39
70	0.85	4.01	0.31

tion where they are no longer mobile and no longer contributing to the dielectric spectrum.²⁵

The curves relating ϵ'' and the applied frequency were analyzed into two absorption regions. The first region was found to be unchanged and could ascribe Maxwell-Wagner effect. The second region ascribes the local molecular motions. The analyses given for polypropylene fumarate crosslinked with NVP and loaded with 60 wt % gypsum before and after immersing in SBF solutions are illustrated graphically in Figure 6. The data obtained from the analyses are listed in Table III.

Comparing Tables II and III it is interesting to find that both conductivity and S_2 decreases, whereas a pronouncing increase in τ_2 is noticed. The increase in τ_2 reflects an increase in the molar volume of the rotating unites due to the formation of apatite structure that takes some ions to crystal formation to become no longer mobile and thus no longer contributing to dielectric spectrum.

To find an expression to distinguish between the amount of apatite structure which is assumed to be formed by immersing the investigated samples in SBF, the relation $(\tau_{\text{aft.}} - \tau_{\text{bef.}})/\tau_{\text{bef.}}$ was calculated and listed in Table III. From this table, it is interesting to notice that the values of $(\tau_{\text{aft.}} - \tau_{\text{bef.}})/\tau_{\text{bef.}}$ increases by the addition of 60% gypsum following the trend NVP > NVP/MMA > MMA. Figure 7 represents the variation of $(\tau_{\text{aft.}} - \tau_{\text{bef.}})/\tau_{\text{bef.}}$ versus NVP content. This figure illustrates the values of $(\tau_{\text{aft.}} - \tau_{\text{bef.}})/\tau_{\text{bef.}}$ for NVP/MMA deviates positively from the line connecting the two individuals. This positive deviation indicates that the properties of polypropylene fumarate crosslinked with NV/MMA are shifted toward those crosslinked with NVP rather than MMA. These results could recommend NVP/MMA to be used in crosslinking polypropylene fumarate

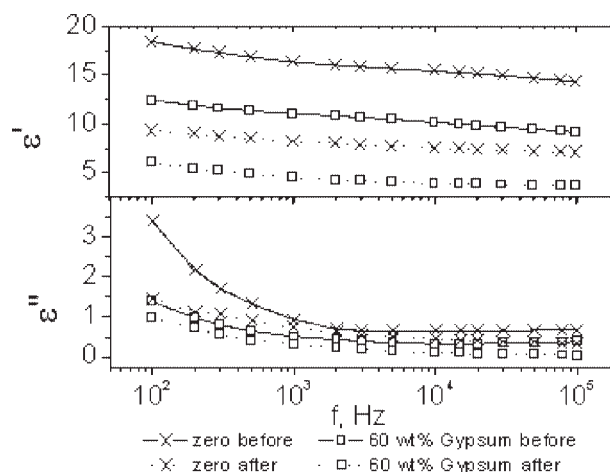


Figure 5 Permittivity ϵ' and dielectric loss ϵ'' for zero PPF/NVP and PPF/NVP loaded with 60 wt % gypsum before and after immersion in SBF solution for 4 weeks.

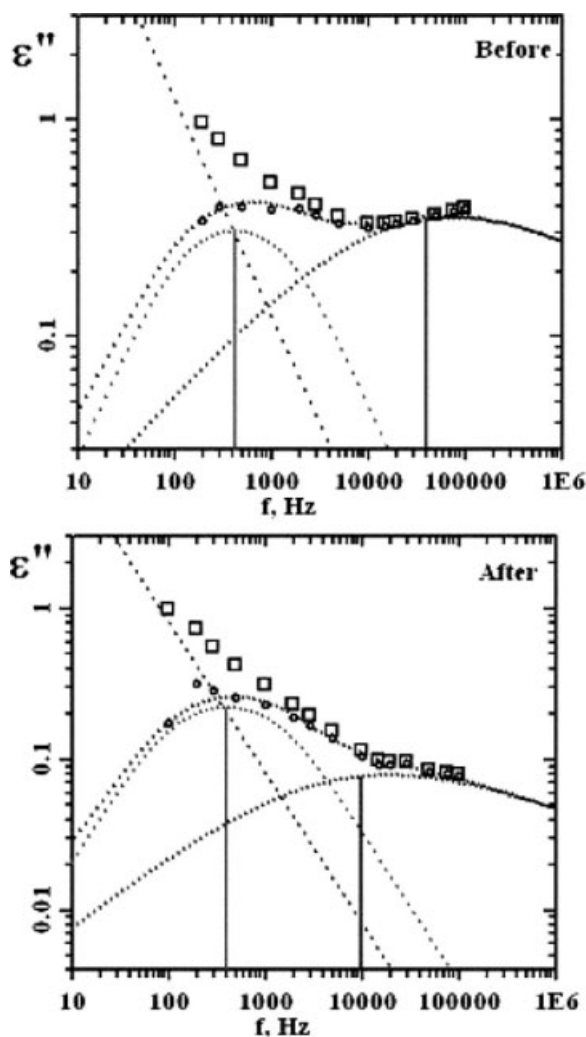


Figure 6 The analyses of ϵ'' data for PPF/NVP loaded with 60 wt % gypsum before and after immersion in SBF solution for 4 weeks. Fitting the experimental data after subtraction of the losses due to dc conductivity with Fröhlich and Havriliak Negami functions.

rather than the expensive monomer NVP and the unrecompensed one MMA.

FTIR investigation

The individual FTIR spectra of gypsum, PPF, and PPF/NVP are represented in Figure 8. The spectrum of the gypsum used in this work is identical to the reported one.²⁶ The spectrum shows two strong absorption peaks at 3545 cm^{-1} and 3405 cm^{-1} , and a weak shoulder at 3243 cm^{-1} . Over the frequency range $2000\text{--}1000\text{ cm}^{-1}$, there are two peaks of medium and strong intensities at 1685 cm^{-1} and 1620 cm^{-1} , respectively. There are assigned to loosely held and strongly held water molecules, respectively, H—O—H bending vibrations.²⁵ There are also very strong doublet at 1142 cm^{-1} and 1115 cm^{-1} due to sulfate group. The spectrum exhibits a strong

couple of bands at 669 cm^{-1} and 602 cm^{-1} due to OS—O bending vibrations.

The IR spectrum of PPF shows an intense strong band at 1730 cm^{-1} characteristic of the stretching frequency of acid and ester carbonyl group. The broad band at 3446 cm^{-1} stand for OH groups and the band at 2960 cm^{-1} is due to stretching frequency of CH_2 . The presence of unsaturation $\text{C}=\text{C}$ in fumarate unit appears at 1643 cm^{-1} .

The spectrum of the mixture of PPF/NVP exhibits the same spectral pattern of pure PPF. The very strong absorption peak at 1730 cm^{-1} referred to ester $\text{C}=\text{O}$ stretch, whereas the unsaturation $\text{C}=\text{C}$ is indicated by the absorption peak at 1645 cm^{-1} . The absorption bands in the $1000\text{--}1300\text{ cm}^{-1}$ region are due to C—O stretching vibrations.²⁷

Polyester composite samples loaded with 60 wt % gypsum were immersed in SBF solution. After 4 weeks immersion, the outer layer of these samples were peeled off and studied by FTIR spectroscopy and illustrated in Figures 9–11.

The major absorption bands of gypsum predominant the spectral features before immersion, whereas the characteristic bands of PPF/NVP composite are represented by 1730 cm^{-1} band with some minor absorption bands in the $1450\text{--}1160\text{ cm}^{-1}$ region as shown in Figure 9. The strong couple of gypsum absorption peaks at 1680 cm^{-1} and 1620 cm^{-1} shifted to 1666 cm^{-1} and 1590 cm^{-1} , respectively. In the $1000\text{--}1500\text{ cm}^{-1}$ range, the very strong doublet absorption peaks specific to gypsum at 1142 cm^{-1} and 1115 cm^{-1} disappeared completely, whereas there are some newly developed absorption peaks at 1425 cm^{-1} , 1167 cm^{-1} , and 1062 cm^{-1} .

Over the spectral region $400\text{--}1000\text{ cm}^{-1}$, there is no evidence for the presence of gypsum since the specific two strong absorption bands at 670 cm^{-1} and 600 cm^{-1} disappeared as well. There is a new medium to strong broad absorption band appeared at 578 cm^{-1} . In addition, there are two medium and weak absorption peaks newly appeared at 875 cm^{-1} and 711 cm^{-1} , respectively.

TABLE III
Dielectric Parameters of the Composites Under Investigations After Immersing in SBF Solution

Gypsum wt%	$\sigma\ \Omega^{-1}\text{ cm}^{-1} \times 10^{11}$	$\tau_2 \times 10^5\text{ s}$	S_2	$(\tau_{\text{aft.}} - \tau_{\text{bef.}})/\tau_{\text{bef.}}$
NVP				
0	6.50	2.90	2.35	2.92
60	4.49	3.51	0.50	3.39
NVP/MMA				
0	6.67	5.02	1.87	1.89
60	3.70	6.39	0.63	2.87
MMA				
0	1.40	6.20	0.72	0.862
60	1.12	10.20	0.35	1.91

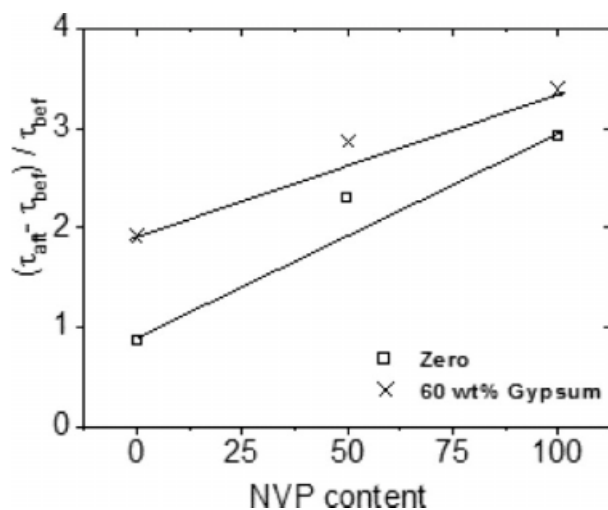


Figure 7 Relation between $(\tau_{\text{aft}} - \tau_{\text{bef}})/\tau_{\text{bef}}$ and NVP content in NVP/MMA mixture.

The strong IR peaks at 1425 cm^{-1} and 1062 cm^{-1} together with the absorption peaks at 875 cm^{-1} and 711 cm^{-1} can be attributed to the carbonate group.²⁷ The absorption peak at 578 cm^{-1} can be assigned to the phosphate group.²⁸ Therefore, the IR results can approve the presence of carbonated apatite in the outer layer formed on the surface of the prepared sample as a result of immersion in the SBF for 4 weeks.

The PPF crosslinked with MMA and loaded with 60 wt % gypsum was examined by FTIR spectroscopy before and after immersion in SBF for 4 weeks (Fig. 10). Careful examination of the spectra reveals that the gypsum absorption bands predominate the spectrum before immersion, whereas the polymer is indicated by medium absorption peak at 1730 cm^{-1} and some minor absorption bands in the region $1450\text{--}1290\text{ cm}^{-1}$. After immersion, the major absorption peaks of the gypsum disappeared, so the polymer absorption bands predominated. On the other hand, some new absorption bands of medium intensity appeared at 1589 cm^{-1} , 1151 cm^{-1} , and 1076 cm^{-1} . Three new absorption peaks of weak intensity appeared at 843 , 711 , and 550 cm^{-1} as a result of immersion in the SBF.

The PPF was crosslinked with MMA/NVP and loaded with 60 wt % gypsum. The obtained FTIR spectra of the samples before and after immersion in SBF for 4 weeks are illustrated in Figure 11. Comparing the spectra before immersion in SBF from Figures 10 and 11 shows that crosslinking of MMA/NVP did not produce obvious change in the molecular structure of the compound, whereas after immersion in SBF for 4 weeks few absorption bands at 1666 cm^{-1} , 1590 cm^{-1} , and 990 cm^{-1} exhibited different intensities. After immersion in SBF, the absorption bands observed at 1076 cm^{-1} , 843 cm^{-1} , 711 cm^{-1} , and 578 cm^{-1} can be considered as good

evidences for the formation of carbonate apatite (Fig. 11).

Mechanical properties

The mechanical behavior under compressive forces was studied through the compressive stress–strain diagrams for the fumarate resin crosslinked with MMA, NVP, and [NVP/MMA (1 : 1 weight ratio)] loaded with three different ratios of gypsum 60, 65, and 70 wt %. The compressive stress–strain diagrams are given in Figure 12. This figure showed that a compressive strength for sample contains 60 wt % gypsum and crosslinked with NVP is 19.6 MPa at % strain at fracture 12.4 and for composites crosslinked with MMA the strength was 10.6 at fracture 11.7. Meanwhile, the compressive strength for

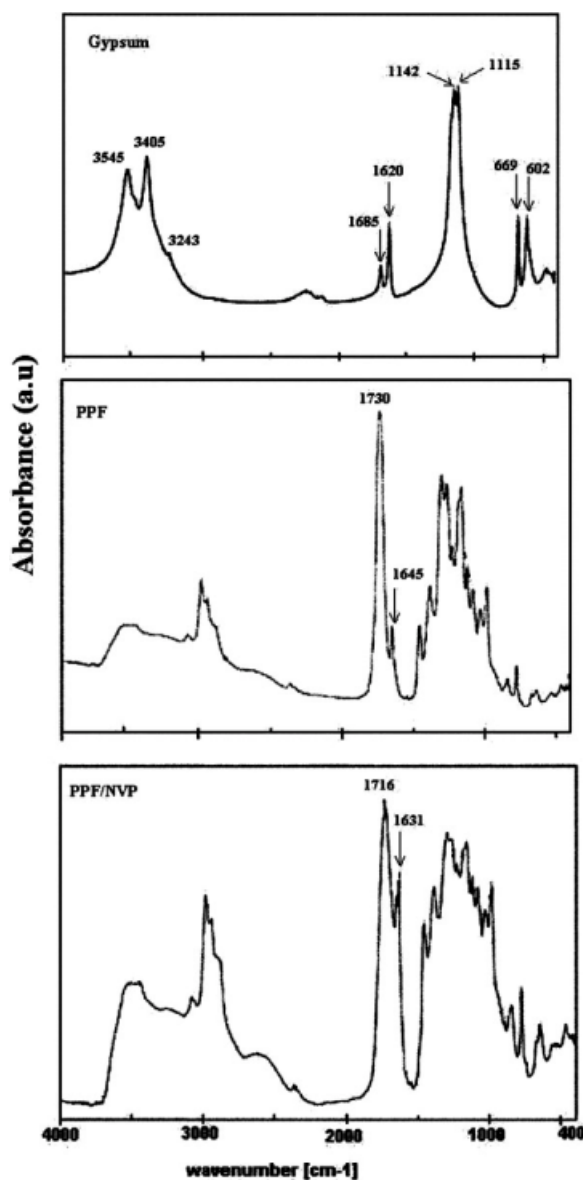


Figure 8 FTIR spectra of gypsum, PPF, and PPF/NVP.

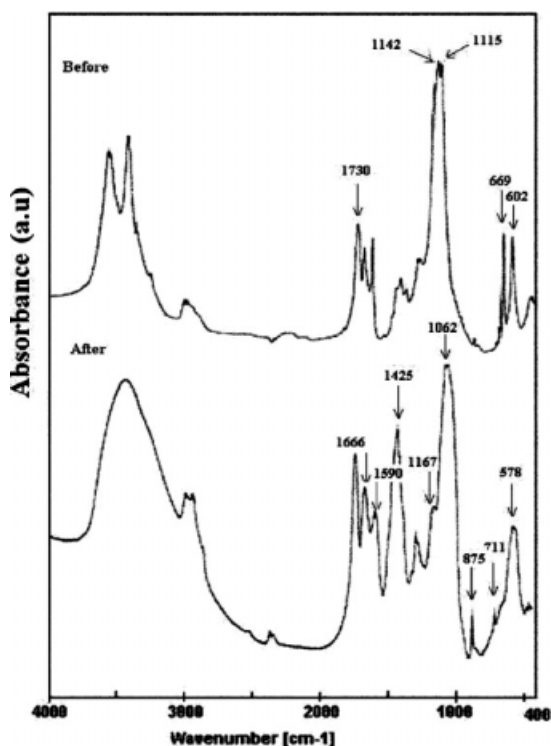


Figure 9 FTIR spectrum of PPF/NPV loaded with 60 wt % gypsum before and after immersion in SBF solution for 4 weeks.

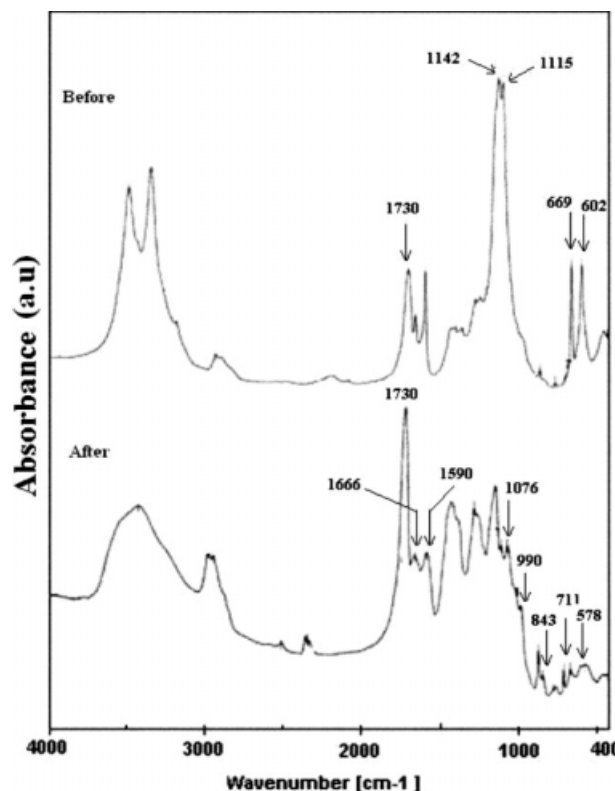


Figure 11 FTIR spectrum of PPF/(NVP/MMA) loaded with 60 wt % gypsum before and after immersion in SBF solution for 4 weeks.

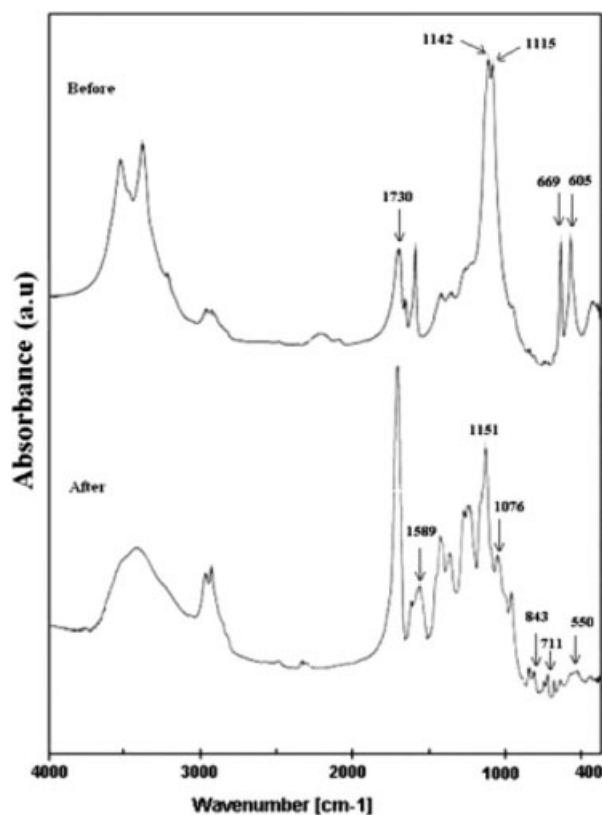


Figure 10 FTIR spectrum of PPF/MMA loaded with 60 wt % gypsum before and after immersion in SBF solution for 4 weeks.

composite crosslinked with NVP/MMA was found to be 15 MPa at % strain 10.3. Also, it is clear that these values decrease by increasing filler content indicating weak mechanical properties. This decrease which was noticed by increasing filler content could be attributed to the in-homogeneity in the specimen which is expected to have place by increasing the percentage of gypsum.

From the earlier data, one can conclude that the best mechanical behavior obtained for samples contains 60 wt % gypsum and the behavior of the composites under investigations follows the order NVP > NVP/MMA > MMA which is the same trend obtained from the dielectric investigations.

The specimens containing 60 wt % gypsum were selected to be studied through the formation of carbonate appetite when immersed in buffer solution for 4 weeks. After immersing in such solutions, the compressive strength was found to increase as shown in Figure 13, whereas the strain at fracture was found to decrease to a value in the order of 6%. The result is considered to be a good evidence for the formation of carbonate appetite.

Biodegradability test

The biodegradability of PPF crosslinked with NVP, MMA, and NVP/MMA loaded with 60 wt %

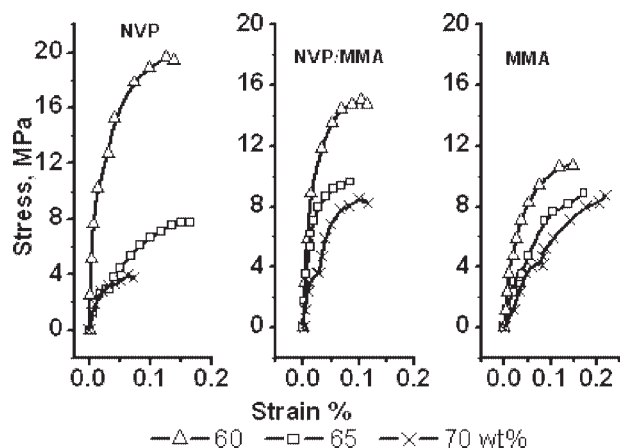


Figure 12 Compressive strength values of PPF cross-linked with various monomers and loaded with different percentages of gypsum.

gypsum is attributed to their ability to undergo hydrolysis to their respective monomeric carboxylic acids and diols. *In vitro* demonstration of biodegradation requires experimental conditions mimicking the physiological characteristics of the living media. Thus, SBF (pH 7.3) was used as *in vitro* medium to provide iso-osmolarity and to neutralize the generated carboxyl groups. The degradation rate of cross-linked fumarate-based polyesters as well as bone cement composites were measured in terms of the weight loss over time of exposure to the SBF solutions as shown in Figure 14. Degradation of PPF crosslinked with NVP is slower than that of MMA and NVP/MMA.

The formation of carbonate apatite, by immersing in SBF solution which is detected by FTIR and confirmed by the dielectric relaxation method, is accompanied by degradation in the composite itself. The

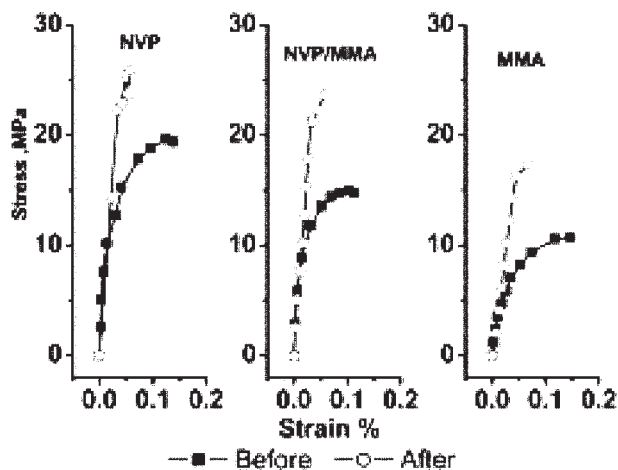


Figure 13 Compressive strength values of PPF cross-linked with various monomers and loaded with 60 wt % gypsum before and after immersing in SBF solution.

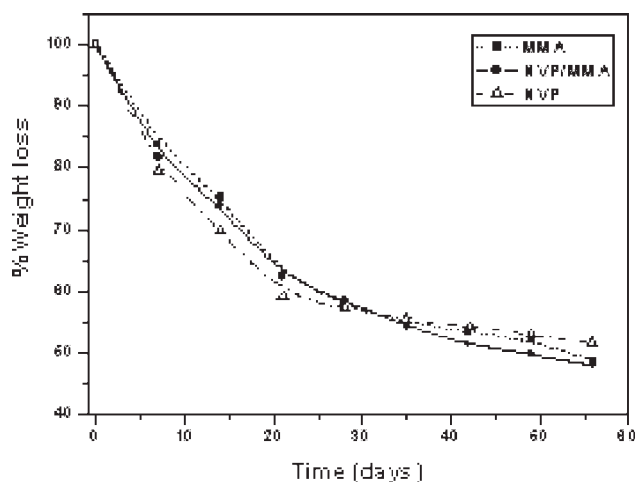


Figure 14 Percentage of the weight loss versus time (days).

weight of the formed apatite is too small when compared with the total loss in weight, Figure 14.

CONCLUSIONS

Polypropylene fumarate as unsaturated linear polyester crosslinked with three different monomers *N*-vinylpyrrolidone (NVP), methyl methacrylate (MMA), and mixture of NVP/MMA (1 : 1 weight ratio) and filled with 60, 65, and 70 wt % gypsum were prepared to be used as bone cements. The study was carried out through the dielectric relaxation investigation in addition to the mechanical properties.

The dielectric data as well as the mechanical ones indicate that 60% gypsum is characterized by the optimum properties rather than the crosslinkers which were found to follow the trend NVP > NVP/MMA > MMA.

Carbonate apatite was found to be formed by immersing these composites in stimulated body fluid SBF solution for 4 weeks. The increase in the relaxation time reflects an increase in the molar volume of the rotating units that takes some ions to crystal formation to become no longer mobile and no longer contributing to dielectric spectrum. The appearance of newly developed absorption peaks through the FTIR spectra is considered to be a good evidence for the formation of such apatite. The biodegradability through the hydrolytic stability in living media in the presence of SBF was measured as the weight loss over time of exposure.

References

- Hosoya, N.; Sato, K.; Arai, T. *Jpn J Conservative Dentistry* 2004, 47, 709.
- Lee, J. W.; Lan, P. X.; Kim, B.; Lim, G.; Cho, D.-W. *J Biomed Mater Res B Appl Biomater* 2008, 87, 1.

3. Lee, K.-W.; Wang, S.; Yaszemski, M. J.; Lu, L. *Biomaterials* 2008, 29, 2839.
4. Fisher, J. P.; Holland, T. A.; Dean, D.; Engel, P. S.; Mikos, A. G. *J Biomater Sci Polym Ed* 2001, 12, 673.
5. Peter, S. J.; Nolley, J. A.; Widmer, M. S.; Merwin, J. E.; Yaszemski, M. J.; Yasko, A. W.; Engel, P. S.; Mikos, A. G. *Tissue Eng* 1997, 3, 207.
6. Kharas, G. B.; Kamenetsky, M.; Simantirakis, J.; Beinlich, K. C.; Rizzo, A. M. T.; Caywood, G. A.; Watson, K. *J Appl Polym Sci* 1997, 66, 1123.
7. Dong, X.; Jong, Gu. P.; Jun, Z. *J Appl Polym Sci* 2006, 103, 2977.
8. Domb, A. J.; Manor, N.; Elmalak, O. *Biomaterials* 1996, 17, 411.
9. Choll, W. K.; Robert, T.; Lichun, L.; Michael, J. M.; Bradford, L. C.; Michael, J. Y. *J Biomed Mater Res A* 2007, 58, 1114.
10. Losquadro, W. D.; Tatum, S. A.; Allen, M. J.; Mann, K. A. *Arch Facial Plast Surg* 2009, 11, 104.
11. Shalumon, K. T.; Jayabalan, M. *J Mater Sci: Mater Med* 2009, 20, 1379.
12. Cai, Z. Y.; Yang, D. A.; Zhang, N.; Ji, C. G.; Zhu, L.; Zhang, T. *Acta Biomater* 2009, 5, 628.
13. Peter, S. J.; Miller, S. T.; Zhu, G.; Yasko, A. W.; Mikos, A. G. *J Biomed Mater Res* 1998, 41, 1.
14. Kempen, D. H.; Lu, L.; Kim, C.; Zhu, X.; Dhert, W. J.; Currier, B. L.; Yaszemski, M. J. *J Biomed Mater Res A* 2006, 77, 103.
15. Shahriar, S.; Hamid, M.; Mohammad, I.; Zimei, R.; Ahmad, J.; Mohammadali, S.; Mohammad, A.; Nima, R. *Acta Biomater* 2009, 5, 1966.
16. Henry, F.; Costa, L. C.; Devassine, M. *Eur Polym J* 2005, 41, 2122.
17. Jayabalan, M. *Int J Biomater* 2009, Article ID 486710.
18. Kokubo, T.; Kushitani, H.; Sakka, S.; Kitsugi, T.; Yamamuro, T. *J Biomed Mater Res* 1990, 24, 721.
19. Abd-El-Messieh, S. L.; Abd-El-Nour, K. N. *J Appl Polym Sci* 2003, 88, 1613.
20. Yuhong Hu, H. R. M.; Etxeberria, A. M.; Fernandez Berridi, M. J.; Iruin, J. J.; Paul, C. P.; Michael, M. C. *Macromol Chem Phys* 2000, 201, 707.
21. Abd-El-Messieh, S. L. *J Mol Liq* 2002, 95, 167.
22. Hill, N. E.; Vaughan, W. E.; Price, A. H.; Davies, M. *Dielectric Properties and Molecular Behaviour*; Van Nostrand: London, 1969.
23. McMorro, B.; Chartoff, R.; Klosterman, D. *SAMPE, Proceedings*, Long Beach, California, May 1, 2003.
24. Havriliak, S.; Havriliak, S. J. *Dielectric and Mechanical Relaxation in Materials*; Hanser Publishers: Cincinnati, 1997.
25. Mohamed, M. G.; Abd-El-Messieh, S. L.; El-Sabbagh, S.; Younan, A. F. *J Appl Polym Sci* 1998, 69, 775.
26. Bohic, S.; Rey, C.; Legrand, A.; Sfihi, H.; Rohanizadeh, R.; Martel, C.; Barbier, A.; Daculsi, G. *Bone* 2000, 26, 341.
27. Paschalis, E. P.; Betts, F.; Dicarolo, E.; Mendelsohn, R.; Bosk, A. L. *Calcif Tissue Int* 1997, 61, 480.
28. Gadaleta, S. J.; Medelsohn, R.; Paschalis, E. P.; Camacho, N. P.; Betts, F.; Boskey, A. L. In *Fourier Transform Infrared Spectroscopy of Synthetic and Biological Apatites: A Review in Mineral Scale Formation and Inhibition*; Amjad, Z., Ed.; Plenum Press: New York, 1995; p 283.